Article

Investigation of Phosphorus Loaded V$_2$O$_5$/ZrO$_2$ Catalysts for the Oxidative Dehydrogenation of Propane (ODH)

Abdellah Benzaouak [1,2,*], Hanane Mahir [2], Adnane El Hamidi [2], Mohamed Kacimi [2]
and Leonarda Francesca Liotta [3,*]

[1]   Laboratory of Spectroscopy, Molecular Modeling, Materials, Nanomaterials, Water and Environment, Environmental Materials Team, ENSAM, Mohammed V University, Rabat 10100, Morocco
[2]   Laboratory of Physical Chemistry of Materials, Catalysis, and Environment, Department of Chemistry, Faculty of Sciences, Mohammed V University, Rabat 10100, Morocco; hanane_mahir@um5.ac.ma (H.M.); a.elhamidi@um5r.ac.ma (A.E.H.); m.kacimi@um5r.ac.ma (M.K.)
[3]   Istituto per lo Studio dei Materiali Nanostrutturati (ISMN)-CNR, Via Ugo La Malfa 153, 90146 Palermo, Italy
[*]   Correspondence: a.benzaouak@um5r.ac.ma (A.B.); leonardafrancesca.liotta@cnr.it (L.F.L.)

Abstract: In this study, V$_2$O$_5$/ZrO$_2$ samples loaded with different wt% of V$_2$O$_5$, ranging between 0% and 20% (wt% = 2.5, 3.6, 7.5, 10, and 20), were prepared and studied in the dehydrogenation of 2-butanol in order to investigate their acid-basic properties and to select the most interesting sample, that was identified in the 3.6 wt%V$_2$O$_5$/ZrO$_2$. Such a catalyst was modified by adding phosphate at different atomic ratios (P/V = 0.5, 1, and 2) and further characterized by XRD, SEM-EDX, ESR, UV-Vis-PIR diffuse reflectance. Tests of catalytic dehydrogenation of 2-butanol were also performed. Then, the so-prepared samples were investigated in the oxidative dehydrogenation (ODH) of propane that represents the reaction of main interest in this study. It has been shown that the introduction of 3.6 wt%V$_2$O$_5$ and phosphate in the zirconia matrix enhances the stability of the tetragonal structure, improves acidity, and promotes ODH activity. Compared to the unpromoted 3.6 wt%V$_2$O$_5$/ZrO$_2$ catalyst, the addition of phosphate increases the overall propane conversion from 12% to 20%, and also the propylene selectivity from 54% to near 64%, in the experimental conditions F$^\circ$C$_{3H8}$/F$^\circ$O$_2$/F$^\circ_{total}$ (cm^3/min): 3.6/1.8/60 at the temperature of 500 °C. The influence of the reaction mixture on the ODH, in particular the oxygen flow rate, was addressed. Highlights: Phosphorus loaded V$_2$O$_5$/ZrO$_2$ catalysts were prepared and investigated in the oxidative dehydrogenation of propane. Addition of V$_2$O$_5$ and phosphorus to ZrO$_2$ stabilized the tetragonal phase with respect to the monoclinic one. Among the prepared V$_2$O$_5$/ZrO$_2$ samples, the most active catalyst corresponds to 3.6 wt% of V$_2$O$_5$/ ZrO$_2$, The addition of phosphorus to 3.6 wt% V$_2$O$_5$/ZrO$_2$ improves acidity and selectivity to propylene. Correlation between catalysts acidity and oxidative dehydrogenation of propane was observed.

Keywords: phosphate; mixed oxides; 2-butanol conversion; oxidative dehydrogenation; ODH; zirconia; vanadia

1. Introduction

Nowadays there is a huge demand for olefins as a feedstock for various industrial applications. The industrial production of olefins is carried out mainly via steam cracking, catalytic cracking and catalytic dehydrogenation processes, which are high energy consuming due to the endothermic nature of the reactions. In addition, catalyst deactivation occurs due to coke formation, and regular regeneration is required, increasing the production costs [1]. Environmental menaces make the production of light olefins via oxidative dehydrogenation of alkanes a more desirable approach than other ordinary methods. Recently, many researchers have focused on these conservative and clean processes [2,3].

Propene production is extremely important in the manufacture of several high-value derivatives. It is the monomer of polypropylene, which is a thermoplastic widely used

in the packaging, automotive, household appliances, sanitary and textile industries. The process of catalytic oxidative dehydrogenation of propane is a promising way to overcome the growing demand for this product. Among the catalysts used for this reaction, there are materials based on alkalis and alkaline earth metals, exhibiting high selectivity; however, they perform only at too high temperatures [4]. In contrast, catalysts based on reducible oxides are performant and can operate at much lower temperatures [5]. However, the low selectivity in propene remains a major handicap for its socioeconomic development [4]. Thus, the study of the production of propene via catalytic propane dehydrogenation is always a challenge [6].

Vanadium oxide is an important catalytic material, having unique characteristics, high catalytic efficiency, and can be used in various chemical processes [7]. However, in practice, it suffers from low stability and poor conductivity, hampering its performance. Thus, several studies have explored the properties of supported vanadium oxide [8–11]. Generally, the catalytic performance in terms of activity or selectivity of vanadia is improved by addition of promoters, while the mechanical properties, thermal stability, and longevity are improved by modifying the support. Indeed, in situ investigations of V_2O_5 supported on the oxides of Al, Ce, Ti, Nb, and Si, by Raman and UV-Visible spectroscopy [12], have shown that the redox process of vanadium species, in the presence of ethane depends on the nature of the support. The reduction of vanadium entities on the surface is easier in the presence of zirconia than on other supports. Other work of these systems in the oxidation of methanol also found that zirconium oxide promotes the reduction of V^{5+} ions [13]. It is reported that the position of the V = O vibration band in Raman spectroscopy has shifted $30 \ cm^{-1}$ towards the low frequencies whatever the support oxide, whereas the same band undergoes practically no shift under the ethane/O_2 reaction mixture [13]. Other studies have been devoted to the influence of the addition of ZrO_2 on the catalytic behaviour of V_2O_5/Al_2O_3 in methanol oxidation. It has been noted that Zirconia improves catalytic performance and exhibits an excellent synergistic effect in terms of reducibility and acidity properties [14].

Many industrial applications of heterogeneous catalysis are based on acidic or basic materials. This character can come either from the support or from the active phase. Whether of the Lewis or Brönsted type, acid catalysts are required as intermediates in reaction mechanisms involving carbocations [15]. In general, all reactions that involve a carbocation intermediate are accompanied by non-selective reactions, leading to coke formation.

The alcohol dehydrogenation reaction is commonly used to study the acid-base and redox properties of the catalysts in their working conditions. They can produce aldehydes and ketones by dehydrogenation preferentially on basic catalysts, while dehydration reaction occurs on acidic sites, producing olefins and ethers products [16,17]. Among the alcohols most used to probe catalyst, there is 2-butanol decomposition. It depends on the catalyst nature, the 2-butanol dehydration leads to 2-butene (cis and trans isomers), and 1-butene formation, while the dehydrogenation leads to the formation of methyl-ethyl ketone [17].

It is worth mentioning that the catalytic activity and selectivity are directly related to the nature and strength of the active sites of the catalysts, which can be designed by modifying the structure and composition of the solid catalysts. This work is in line with this logic of understanding the interaction between ZrO_2, V_2O_5, and phosphate solids to contribute to the modelling of the properties in the oxidative dehydrogenation reaction of propane.

The present work aims to contribute to the comprehension of C-H bond activation, in the oxidative dehydrogenation of propane, by phosphorus modified vanadium supported on zirconia system, known to be efficient in partial oxidation reactions. Phosphorus addition to the vanadia–zirconia system modifies the composition and enhances the catalytic performance of this system. Before this test, a good physicochemical characterization, by XRD, SEM, ESR, UV-Vis-PIR diffuse reflectance, was carried out, accompanied by an investigation of acid-base and redox properties by using 2-butanol dehydrogenation as

probe reaction. The evaluation of catalytic performances in the oxidative dehydrogenation of propane and 2-butanol was carried out.

2. Results and Discussion

2.1. Butanol Dehydrogenation over V_2O_5/ZrO_2

The 2-butanol dehydrogenation reaction was used as a reaction probe to highlight the acid-base and redox properties of catalysts [18–21]. In the absence of oxygen, the reaction leads to the formation of butanes by 2-butanol dehydration and methyl ethyl ketone (MEK) or butanone by dehydrogenation. The product selectivity reveals the nature of the sites. Thus, the formation of butenes is related to acidic sites, while the formation of MEK is related to basic sites. Moreover, by operating in the presence of oxygen, the resulting reaction is the oxidative dehydrogenation of 2-butanol, producing MEK on redox sites [22]. Figure 1 presents the catalytic activity in 2-butanol dehydrogenation over V_2O_5/ZrO_2 samples as a function of vanadium contents at 205 °C, using a reaction mixture of air and 2-butanol. In N_2 and 2-butanol mixture, the V_2O_5/ZrO_2 catalysts show the formation of approximately 5% and 2.5% of butenes and methyl ethyl ketone (MEK) produced via dehydrogenation and dehydration, respectively (data not shown). In air–butanol mixture, MEK production increases with the vanadium content, reaches a maximum of 40% at 3.6 wt% V_2O_5/ZrO_2, and then suddenly decreases until 10% V_2O_5/ZrO_2, beyond that it does not change significantly. Conversely, the 2-butanol conversion into butenes increases by increasing vanadium content and reaches a constant conversion value of around 50% for 7.5% V_2O_5/ZrO_2. Such value remained stable by increasing the vanadia content up to 10 and 20 wt%, suggesting that a V_2O_5 multilayer is formed on the catalyst surface [23].
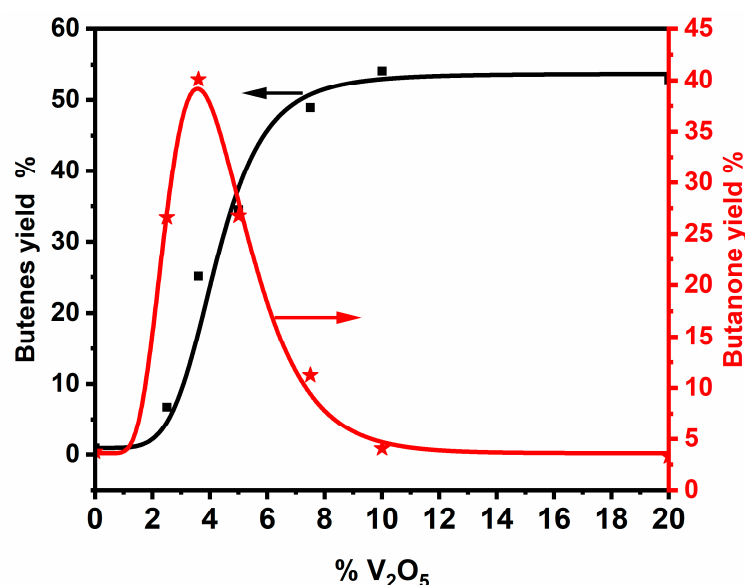

Figure 1. Evolution of the butenes and butanones yields at steady state depending on the V_2O_5 content (wt% = 2.5, 3.6, 7.5, 10, and 20) for a reaction mixture air + 2-butanol at 205 °C.

Figure 2 illustrates the variation of turnover frequency in Butenes (TOFene) and butanones (TOFone) products depending on the vanadium content. It is noticed that TOF increased with the increase of V_2O_5 content, reaches the maximum, and then decreases. The most active catalyst in dehydrogenation is the 3.6 wt% V_2O_5. This result is in agreement with the literature because, at around such composition, it is reported that vanadium forms a monolayer [24].
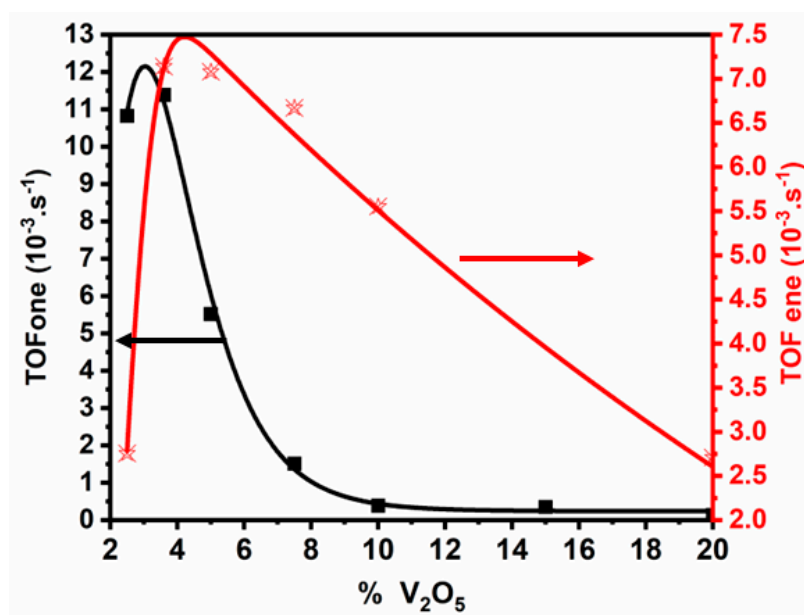
Figure 2. Turnover frequency (TOF) variation depending on the vanadium content (wt% = 2.5, 3.6, 7.5, 10, and 20) at 205 °C under reaction mixture air + 2-butanol.

2.2. Materials Characterization of the 3.6 wt%V_2O_5/ZrO_2 and Phosphate Loaded Catalysts at Different P/V Ratios

Figure 3 illustrates the XRD patterns of the 3.6 wt%V_2O_5/ZrO_2 and phosphate loaded samples. It is shown that the prepared ZrO_2 oxide as reference is present in two crystalline phases, the monoclinic (PDF-00-065-0687; P21/a) and tetragonal (PDF-00-017-0923; P-4m2) ones [25]. After addition of 3.6 wt%V_2O_5, the formation of the tetragonal phase was promoted. Then, in the phosphate loaded samples, the peaks of the monoclinic ZrO_2 decreased in intensity, whereas those of the tetragonal phase remained unchanged. This result is in agreement with those of the literature [26]. No additional characteristic peaks of vanadium oxides or phosphate phases were detected, suggesting high dispersion on the catalyst surface.
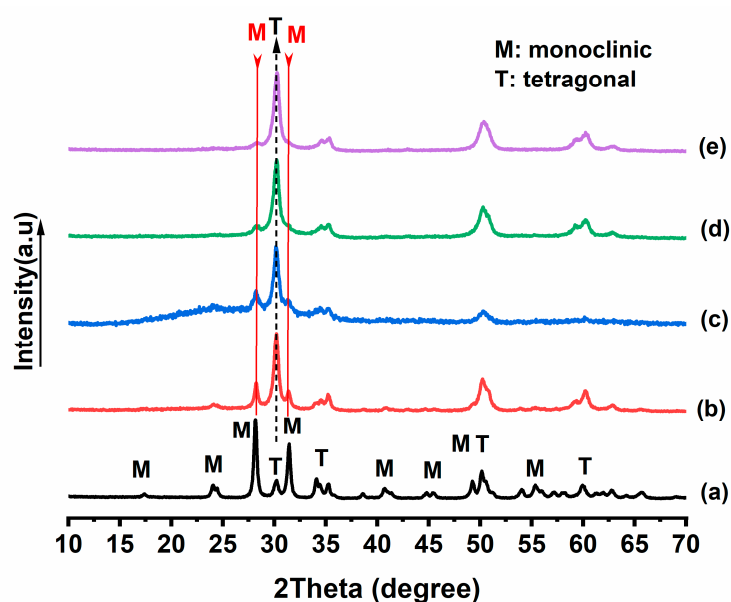

Figure 3. XRD patterns of 3.6 wt%V_2O_5//ZrO_2 and P loaded catalysts at different P/V ratio (**a**) ZrO_2, (**b**) 3.6 wt%V/ZrO_2, (**c**) P/V = 0.5, (**d**) P/V = 1, (**e**) P/V = 2.

The morphological properties of the 3.6 wt%V_2O_5/ZrO_2 and phosphate loaded catalysts were investigated by N_2 adsorption–desorption isotherms. Values of the specific surface area (SSA), pore size distribution and pore volume are listed in Table 1. Referring to IUPAC classification, the obtained isotherms are classical type IV, showing a typical hysteresis of mesoporous materials (see Figures S1–S5). The pore size distribution is shown in Figures S6 and S7, where ZrO_2 and 3.6 wt%V_2O_5/ZrO_2 and P loaded 3.6 wt%V_2O_5/ZrO_2 catalysts at different P/V ratios are compared.

Table 1. Specific surface area SSA (m^2/g) of ZrO_2, 3.6 wt%V_2O_5/ZrO_2 and P loaded samples at different P/V ratios.

Samples	SSA (m^2/g)	Mean Pore Radius (nm)	Pore Volume (cm^3/g)
ZrO_2	5.6	8.81	0.047
3.6 wt%V_2O_5/ZrO_2	16.1	3.96	0.030
P/V = 0.5	43.0	2.15	0.050
P/V = 1	33.6	2.17	0.034
P/V = 2	14.7	3.37	0.020

For comparison, pure ZrO_2 was also analysed. It is interesting to note that the SSA values increase from 5.6 m^2/g (unpromoted ZrO_2) to 16.1 m^2/g (3.6 wt%V_2O_5/ZrO_2), and a further increase occurs by adding phosphate at P/V = 0.5 (43 m^2/g) and at P/V = 1 (33.6 m^2/g). At P/V equal 2, the specific surface area again decreased to a value as low as the starting 3.6 wt%V_2O_5/ZrO_2 catalyst. Among the listed samples, ZrO_2 oxide was characterized by high mean pore size distribution (8.81 nm) and high pore volume (0.047 cm^3/g). The 3.6 wt%V_2O_5/ZrO_2 and phosphate loaded samples exhibited mean pore size smaller than pure zirconia (2.15–3.96 nm) with pore volume ranging between 0.02–0.05 cm^3/g. On the basis of the so far reported data, it can be surmised that depositing 3.6 wt%V_2O_5 over ZrO_2 modifies the surface properties and porosity of parent oxide producing higher specific surface area and a new porosity with lower pore diameter than zirconia. The addition of phosphate further modifies the surface morphology, with an increased specific surface area for P/V = 0.5 and 1 and generating a new porosity centred at around 2.1. At P/V = 2, agglomeration of phosphate species likely occurs and consequently a decreased surface area and pore volume were observed.

Figure 4 displays the FT-IR spectra of various catalysts prepared in the P-V-ZrO_2 system. The band at 1600 cm^{-1} is assigned to the H-O-H stretching vibration. The located band at 3390 cm^{-1} can be assigned to the water molecule [27]. After the addition of phosphate ions, the spectra also show a large band located between 893 and 1300 cm^{-1} that corresponds to the bending vibration of V-O-P, the stretching vibration of V-O-V and the stretching vibration of V^{5+} = O [27]. Distinct narrow vibrational bands characteristic of Zr-O of monoclinic zirconia were observed in the 400–850 cm^{-1} region [28]. These bands become broad and interfered when vanadium and phosphorus are added, based on the evolution of the XRD patterns, this is probably due to the formation of the tetragonal phase of ZrO_2.

Figure 5 shows the UV-Vis-NIR diffuse reflectance spectra of the 3.6 wt%V_2O_5/ZrO_2 and phosphate loaded samples with P/V = 0.5, 1, and 2. We noticed that the spectra present the same profile. They present a broadband, between 190 and 550 nm, assigned to the charge transfer between the full oxygen orbital and the empty V^{5+} orbital without forgetting the $Zr^{4+} \rightarrow O^{-2}$ charge transfer. After loading phosphate, a less intense absorption peak has been located around 621 nm for P/V ratios equal to 0.5 and 2; however, it disappears for the value of 1. This absorption band is due to the d-d transitions of V^{4+} probably of vanadyl VO^{2+} ions reduced from V^{5+}, which shows that some of the V ions are in a reduced state (see ESR) [29,30]. However, the disappear of this band for P/V = 1 could be due to the absence of VO^{2+} ions. The quantity of these ions seems quite small if we take into account the intensity of the corresponding band. It should be noted that the attribution of bands is often complicated by the contribution of the support oxides [31]. It has been reported

that the charge transfer band of V^{5+} ions is located around 400 nm [32]. The band of d-d transitions of V^{4+} and V^{3+} ions appear between 333 and 1000 nm. It should be noted that there is no direct correlation between P/V ration and V^{4+} presence.
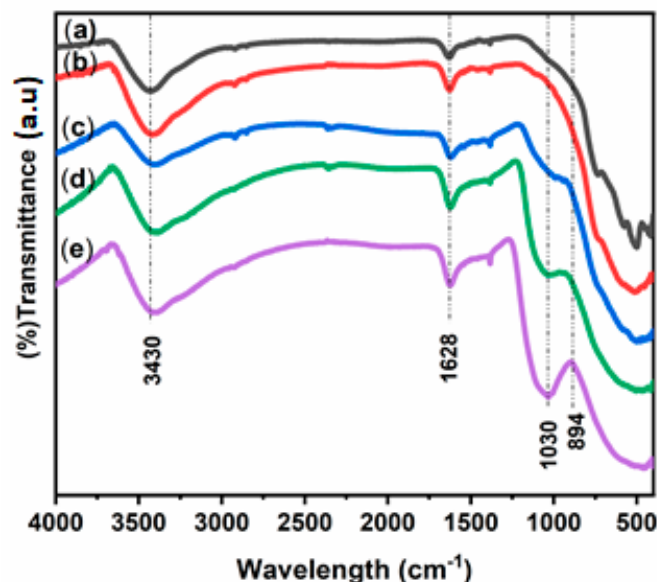

Figure 4. FT-IR spectra of 3.6 wt%V_2O_3/ZrO_2 modified P depending on P/V value (**a**) ZrO_2, (**b**) 3.6 wt%V_2O_5/ZrO_2, (**c**) P/V = 0.5, (**d**) P/V = 1, (**e**) P/V = 2.
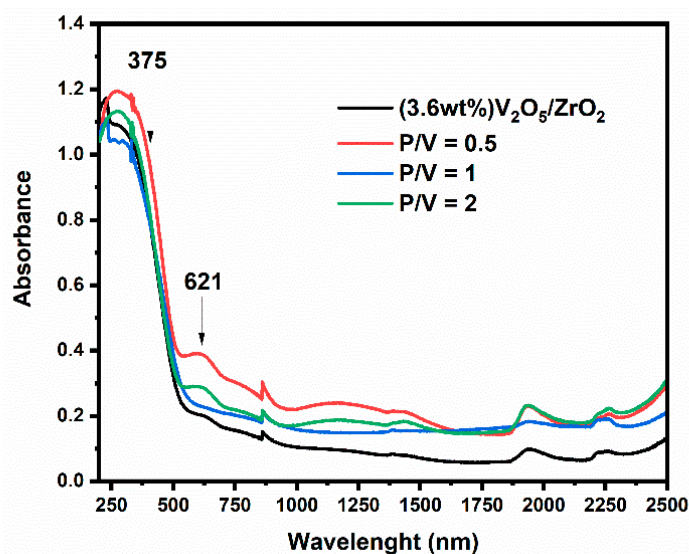
Figure 5. UV-Vis-NIR Spectra of 3.6 wt%V_2O_5)/ZrO_2 modified by phosphate depending on P/V.

The electron spin resonance (ESR) spectroscopy is very sensitive to the environmental symmetry and oxidation state of Vanadium cations, but only for V^{4+} (d^1), which is paramagnetic while it is not for V^{5+} (d^0). The ESR spectrum of the 3.6 wt%V_2O_5/ZrO_2 and phosphate loaded samples is shown in Figure 6. It includes a signal with a hyperfine structure of very low intensity, in agreement with the low concentration of V^{4+} in the sample and the results obtained by the spectroscopies IR and UV-visible. The spectrum of the 3.6 wt%V_2O_5/ZrO_2 loaded phosphate samples also consists of a unique signal different from that observed in the absence of phosphate.
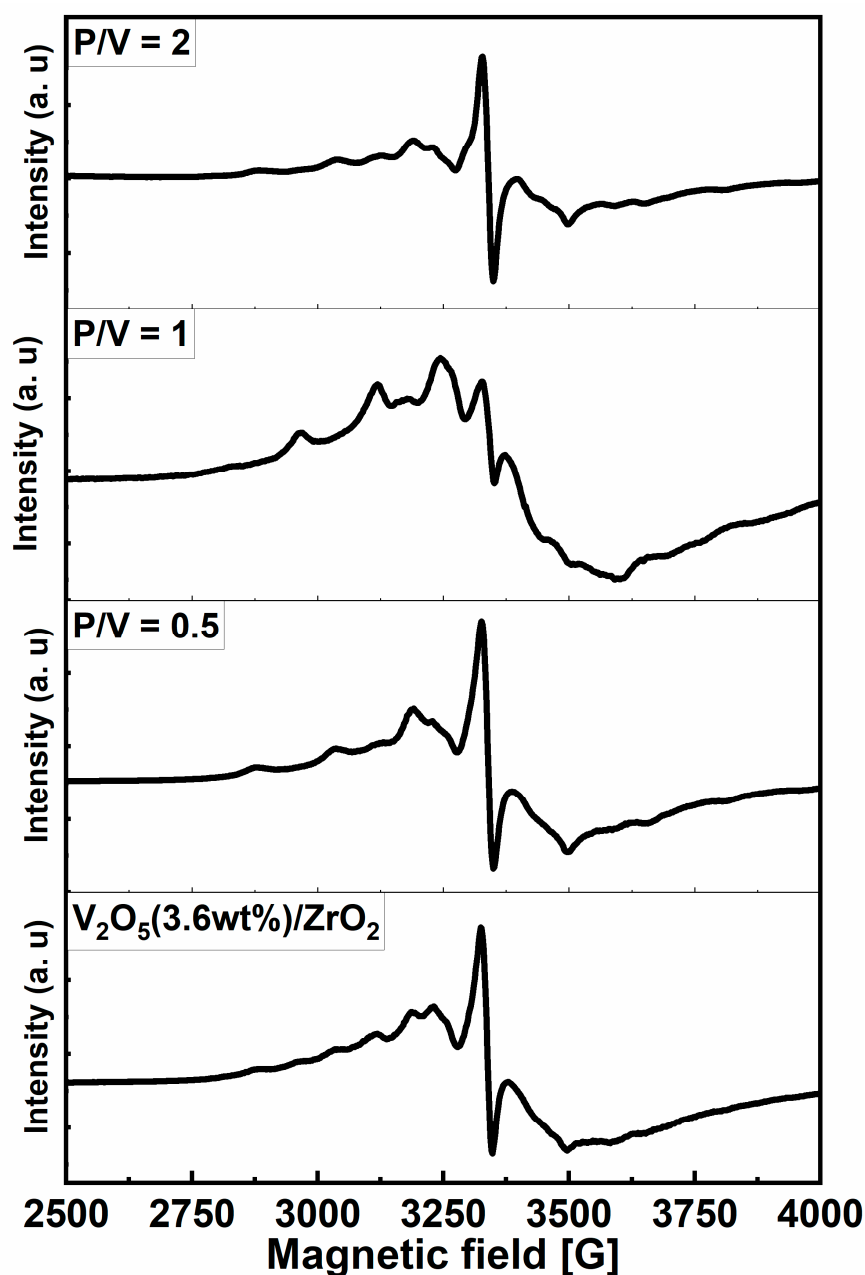
Figure 6. Electron spin resonance (ESR) spectroscopy in liquid N_2 for phosphate modifying 3.6 wt%V_2O_5/ZrO_2 catalysts depending on P/V.

The observed signals presenting hyperfine structures and corresponding to two V^{4+} species in two different environments [27]. The signal obtained with 3.6 wt%V_2O_5/ZrO_2 corresponds to an octahedral symmetry as in VO_2. The signal obtained in the presence of phosphate attributed to V^{4+} ions in a lower symmetry, probably tetrahedral as in V_2O_4. It is difficult to calculate the corresponding g-factors. The 3.6 wt%V_2O_5/ZrO_2 phosphate loaded with P/V equal to 0.5 and 2 samples lead to an ESR signal characterized by a well-resolved hyperfine structure. It is attributable solely to vanadyl ions, in agreement with the results of UV-visible spectroscopy, which have shown that an enrichment of the sample in phosphorus is accompanied by a reduction of V^{5+} ions to V^{4+} by an increase in their number.

The surface and morphology of studied catalysts has been investigated by scanning electron microscopy (SEM) imaging and EDX analysis for the elemental mapping distribution. The photos from this technique are illustrated in Figure 7. It has been observed

that the particle size is not uniform; however, the phosphorus and vanadium elements are well distributed. EDX has also been used to confirm the composition of the catalysts, in particular of the P loaded 3.6%V_2O_5/ZrO_2 with P/V = 1 (Figure 8), which is the most active in oxidative dehydrogenation of propane.
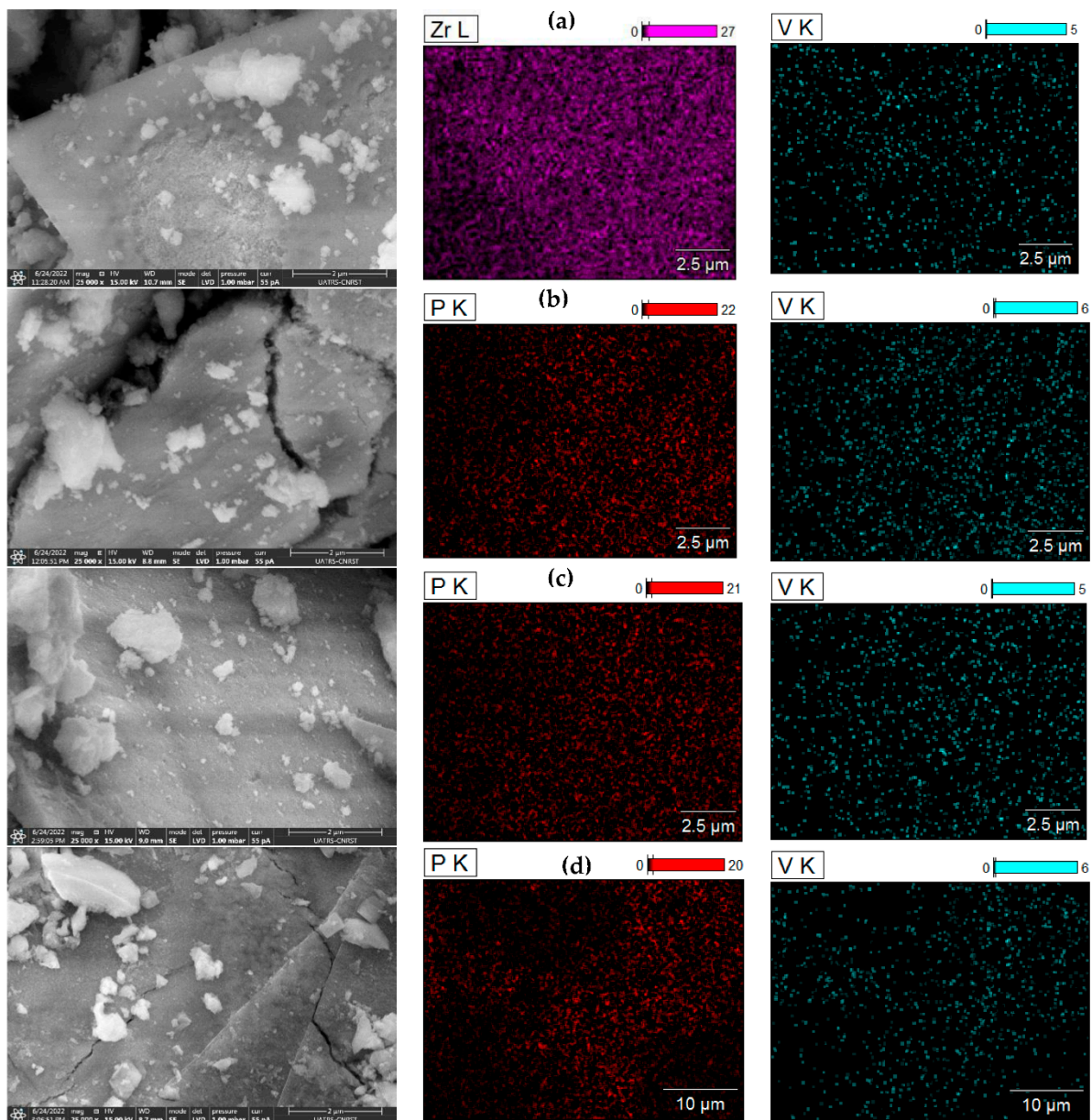

Figure 7. SEM and mapping images of the 3.6 wt%V_2O_5/ZrO_2 loaded phosphate catalysts at different P/V ratio: (**a**) 3.6 wt%V_2O_5/ZrO2; (**b**) P/V = 0.5; (**c**) P/V = 1; and (**d**) P/V = 2.
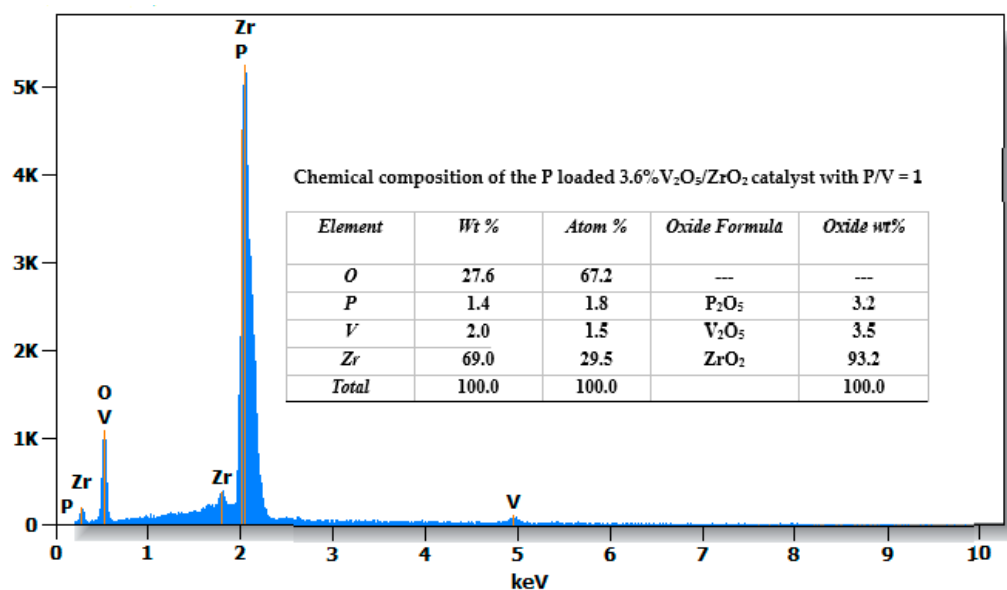
Figure 8. EDX spectrum and chemical composition of P loaded 3.6 wt%V_2O_5/ZrO_2 catalyst with P/V = 1.

2.3. Catalytic Activity

2.3.1. Acid-Basic and Redox Properties of Phosphorus-Modified V_2O_5/ZrO_2

The phosphates effect on the catalytic behaviour of V_2O_5/ZrO_2 was justified according with the literature where the importance of the phosphate in industrial catalysis is highlighted [33]. Generally, phosphorus is added to adjust the acid-base properties of catalysts. It should be noted, in this regard, that the phosphorus compounds of vanadium play an important role in several catalytic processes [34]. Figure 9 displays the butenes and MEK formation, respectively, in 2-butanol dehydrogenation reaction over P modified V_2O_5 (3.6 wt%)/ZrO_2 catalysts at different P/V ratios.
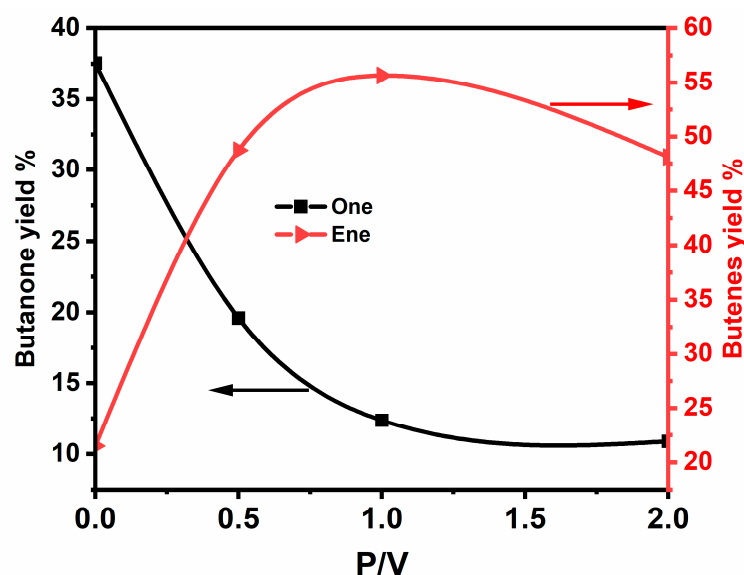

Figure 9. Catalytic activity of P modified V_2O_5 (3.6 wt%)/ZrO_2 catalysts in air mixture depending on P/V ratio in butenes and butanone yield.

The obtained results describe the variation of butanone and butenes yields versus P/V ratio of 0, 0.5, 1 and 2. As mentioned above, 2-butanol dehydration and dehydrogenation reactions give some information on the surface acidity, basicity and redox properties,

respectively. It has been found that the introduction of phosphate promotes the formation of butenes and hence improves the surface acidity. In contrast, the dehydrogenating activity decreases with increasing the P/V ratio.

It should be noted that the focus has been on the dehydrogenation of 2-butanol in the presence of oxygen, since the reaction investigated later in this work is the oxidative dehydrogenation.

In order to compare the catalyst performances, the TOF was used to evaluate the impact of adding phosphate to 3.6 wt%V_2O_5/ZrO_2. Figure 10 shows the TOF of both dehydration (TOFene) and dehydrogenation (TOFone) reactions depending on the P/V ratio as products of 2-butanol conversion. It has been observed that the TOF increases when the P/V ratio increases, attaining a maximum value for P/V = 1 then start to decrease. However, for the dehydrogenation activity, it decreases monotonically when the P/V ratio decreases, and it stabilizes at the value of P/V = 1 ratio, indicating a moderation of the oxidation sites of the alcohol.
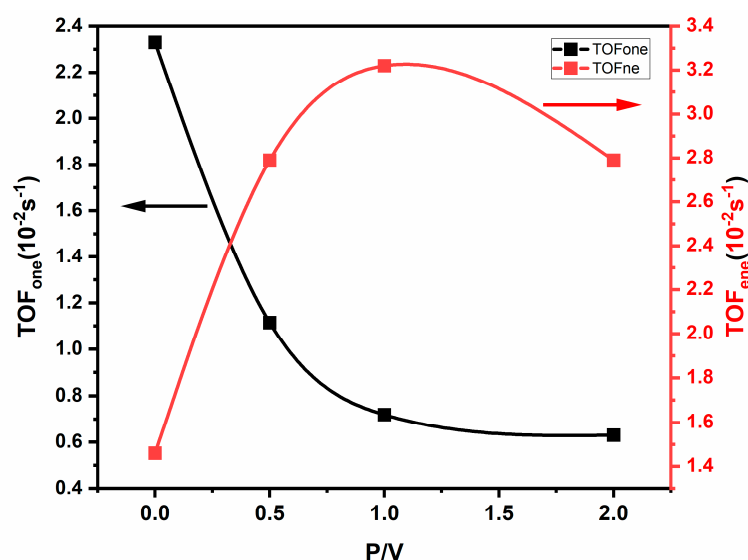

Figure 10. TOF variation of modified V_2O_5 (3.6 wt%)/ZrO_2 catalysts in air mixture depending on P/V ratio in butenes (ene) and butanone (one) yields.

From these results, it seems obvious that the introduction of phosphate modifies the textural properties of the solid. Since this modification moderates the strength of alcohol oxidation sites, it might be beneficial in other reactions such as the oxidative dehydrogenation of alkanes [27].

2.3.2. Oxidative Dehydrogenation (ODH) of Propane

The oxidative dehydrogenation of propane has been completed over prepared catalysts (wt%V_2O_5/ZrO_2). Figure 11 shows the global conversion of propane at different reaction temperatures versus the vanadium content (wt% = 2.5, 3.6, 7.5, 10, and 20). The conversion of propane increases with the vanadium content until it reaches a maximum, which shifts from about wt% = 3.6. When the reaction temperature increases from 450 to 550 °C, the conversion increases with the temperature. However, the propene yield varies from 7 to 9% for the same vanadia content and temperature range (Figure 12).
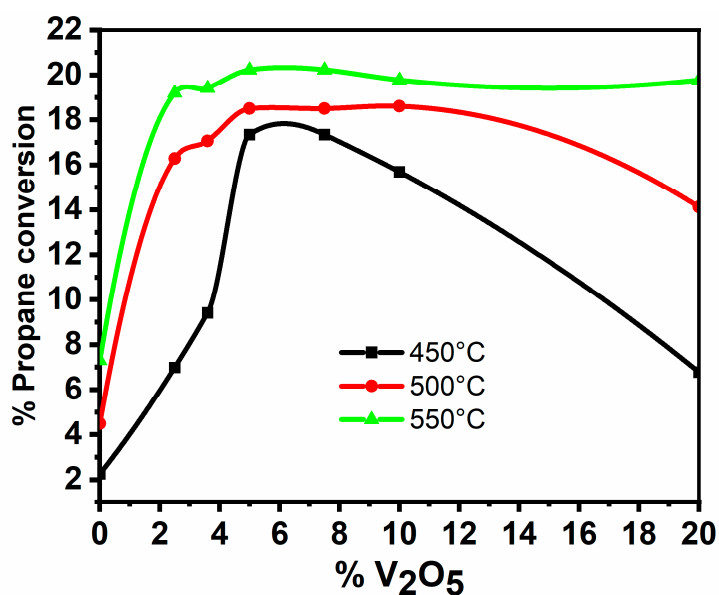
Figure 11. Evolution of the propane conversion as a function of the V_2O_5 content and temperature for a reaction mixture air and propane.
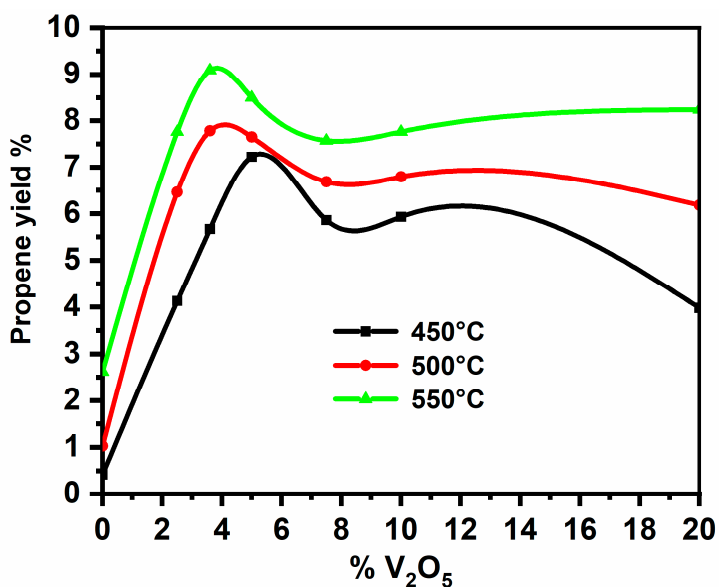

Figure 12. Evolution of the propene yield as a function of the V_2O_5 content and temperature for a reaction mixture air and propane.

Figure 13 displays the catalytic activity obtained over 3.6 wt%V_2O_5/ZrO_2 modified by phosphates ions. As seen, the obtained results improve the propane conversion by showing a beneficial effect of the addition of phosphates on the conversion of propane and propene yield (Figure 14). This behaviour being more evident for P/V = 1, after that the activity of P/V = 2 declines to a comparable activity without phosphate.
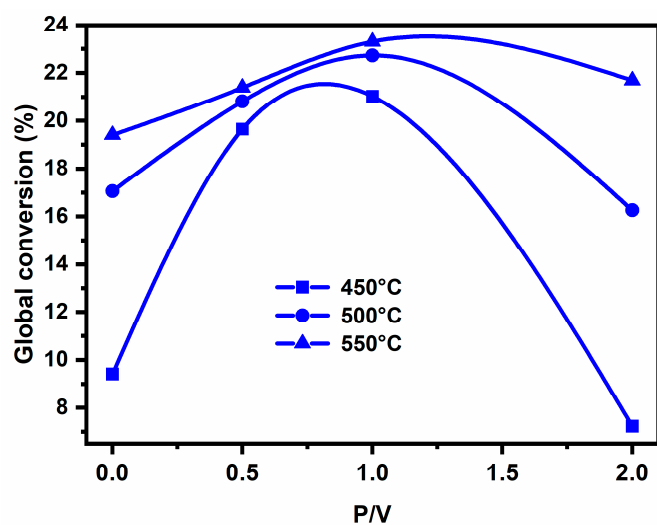
Figure 13. Conversion of propane depending on the reaction temperature and P/V ration in 3.6 wt% V_2O_5/ZrO_2.
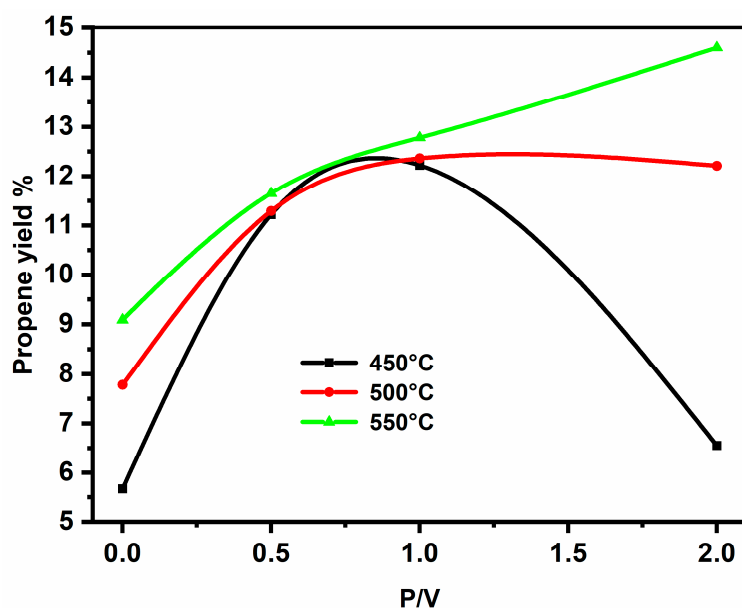

Figure 14. Propane yield depending on the reaction temperature and P/V ration in 3.6 wt% V_2O_5/ZrO_2.

Figure 15 illustrates the variation of propene selectivity of the 3.6 wt%V_2O_5/ZrO_2 modified phosphate versus the reaction temperature and P/V ratio. It is worth noting that for propane ODH, achieving high propene selectivity at high propane conversion is still a challenge, due to the favourable combustion of propene compared to propane ODH [5]. It has been observed that the catalyst prepared at P/V = 1 composition presents a stable average selectivity around 60% regardless of the temperature, while the other materials show a very variable selectivity depending on the temperature and also on the composition, it decreases with increase of phosphate ions and temperature. The catalytic performance as a function of phosphate addition and temperature was evaluated by TOF of propene yield (Figure 16). It found that the catalyst prepared at composition of P/V = 1 in solid 3.6 wt%V_2O_5/ZrO_2 phosphate loaded shows the best performance for all the explored temperatures except for the temperature 550 °C.
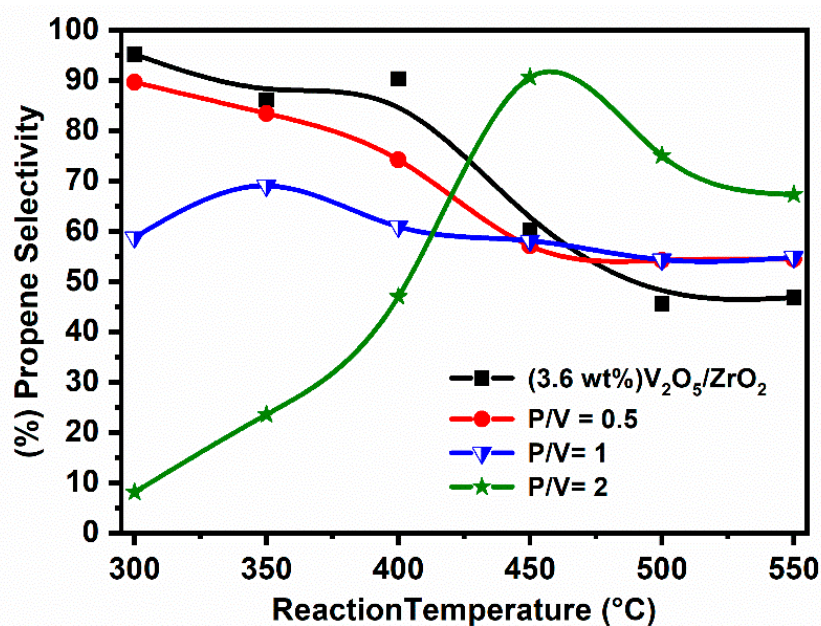
Figure 15. Variation of propene selectivity with reaction temperature and composition.
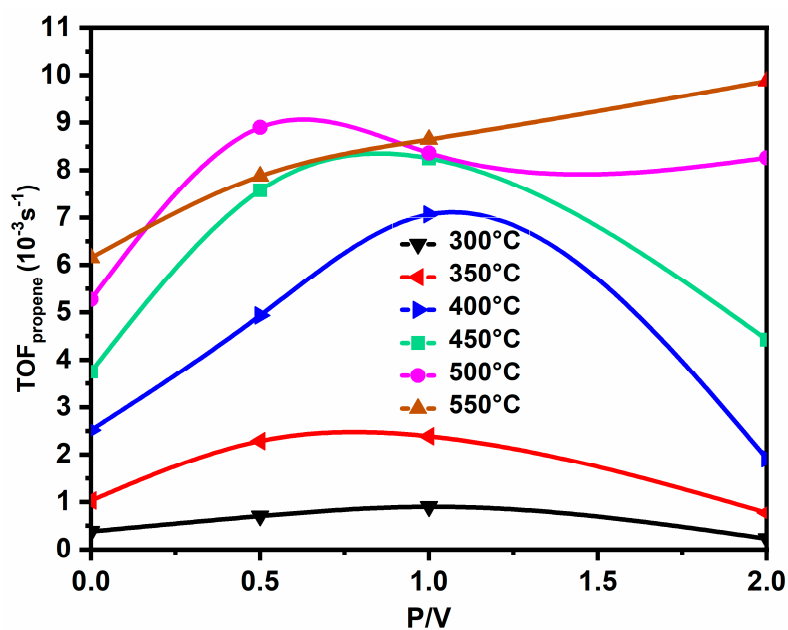

Figure 16. Propene yield TOF variation of 3.6 wt%V_2O_5/ ZrO_2 modified phosphate catalysts in air mixture depending on P/V ratio and temperature.

This variability of selectivity versus overall propane conversion has been distinctly observed (Table 2) when following the effect of the reaction mixture at 550 °C on the catalytic activity for the P/V = 1 phosphate modified V_2O_5(3.6 wt%)/ZrO_2 phase.

Table 2. Comparison of activity and selectivity to propene at 500 °C of 3.6 wt%V_2O_5/ZrO_2 and at P/V = 1 catalyst depending on the reaction mixture.

Operating Conditions	Global Conversion%		Propene Yield%		Propene Selectivity%	
$F°C_{3H8}/F°_{O2}/F°_{total}$ (cm³/min)	3.6 wt%V_2O_5/ZrO_2	P/V = 1	3.6 wt%V_2O_5/ZrO_2	P/V = 1	3.6 wt%V_2O_5/ZrO_2	P/V = 1
3.6/0.9/60	8.92	17.54	5.91	5.31	66.25	30.27
3.6/1.8/60	12.42	20	6.49	12.67	53.82	63.35
3.6/3.6/60	13.41	31.95	6.74	11.99	50.24	37.52
3.6/7.2/60	9.25	53.66	4.81	9.12	51.95	16.99
3.6/1.8/30	17.95	17.56	8.72	12.19	48.58	69.38
3.6/1.8/90	9.34	12.82	4.7	7.55	50.29	58.89
3.6/1.8/120	10.11	14.36	3.45	6.64	34.14	46.23

F°: inlet Flow.

Figure 17 reports the correlation between propene production and the increase in catalyst acidity expressed by the dehydration of 2-butanol. It was found that the highest TOF corresponds to the production of butenes, during the decomposition of 2-butanol, and to the production of propene by the ODH of propane. Such correlation is also observed between the stabilization of the tetragonal structure and the improvement of the acidity of the catalyst surface.
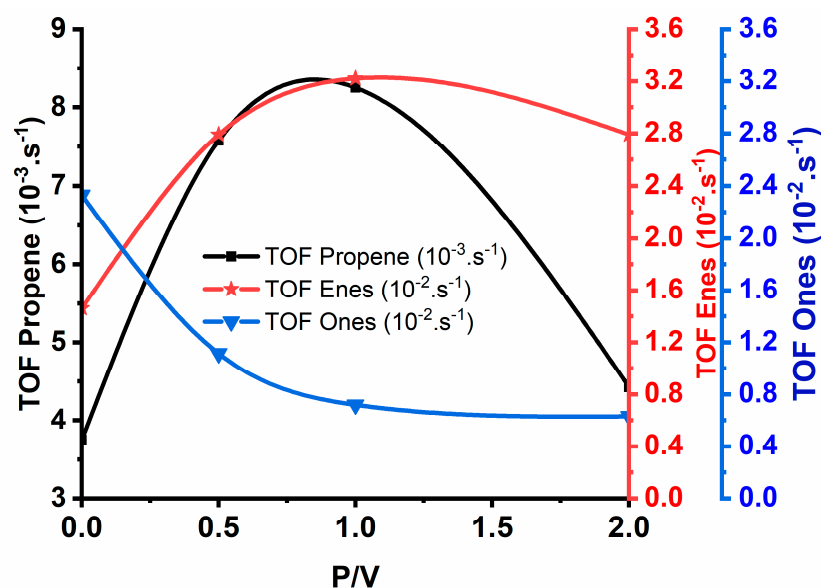
Figure 17. TOF variation as a function of the P/V ratio for the production of propene at 550 °C and for butenes and butanones yields in 2-butanol decomposition at 205 °C in the presence of oxygen.

The V-O-V/V-O-Zr and V = O sites play a critical role in the ODH reaction of propane [35–37]. In this regard, J.J. Ternero-Hidalgo et al., in their work [38] have demonstrated that the oxygen sites of the V-O-V and V-O-Zr bridges are more active than the V = O terminal bonds. In our work, it has been found that there is indeed the presence of the vanadyl VO^{2+} ions, characterized by the terminal V = O, in all the phosphate-modified catalysts, excluding the composition prepared at the P/V = 1 ratio. However, this catalyst shows the highest activity compared to all the 3.6 wt%V_2O_5/ZrO_2 loaded phosphate catalysts, supporting the conclusion of the authors above mentioned. In order to check the sustainability of the prepared catalysts, EDX analyses on the samples recovered after 2-butanol decomposition reaction at 550 °C have been carried out, and any leaching of the active components was excluded.

3. Experimental

The HNO$_3$, Ammonium metavanadate (NH$_4$VO$_3$, $\geq$99.0%, Merck & Co., Darmstadt, Germany), di-Ammonium hydrogen phosphate ((NH$_4$)$_2$HPO$_4$, $\geq$99.0%), Zirconium oxide dichloride octahydrate (lump; 99.9%, Alfa, Kandel, Germany) (ZrOCl$_2\cdot$8H$_2$O), and 2-butanol were purchased from Merck group (Darmstadt, Germany) and Sigma-Aldrich (Saint Louis, MO, USA). All products were used without any additional purification.

3.1. Catalyst Preparation

The V$_2$O$_5$/ZrO$_2$ samples with different V$_2$O$_5$ contents (wt% = 2.5, 3.6, 7.5, 10, and 20) were prepared from the mixture of a solution of ZrOCl$_2\cdot$8H$_2$O and specific amounts of NH$_4$VO$_3$ heated to 90 °C. A solution of HNO$_3$ was added as precipitating agent and the pH was adjusted at 2. The mixture thus obtained was maintained at 90 °C for 1 h and then dried in an oven at 120 °C. The ZrO$_2$ reference was also prepared from ZrOCl$_2\cdot$8H$_2$O using the same protocol. The obtained solids were then calcined in air at 550 °C for 12 h. Phosphorus-modified 3.6 wt% V$_2$O$_5$/ZrO$_2$ catalysts with ratio P/V = 0.5, 1 and 2 were prepared as above reported by adding, at 90 °C, the specific amounts of precursor (NH$_4$)$_2$HPO$_4$ to the reaction mixture used to prepare 3.6 wt%V$_2$O$_5$/ZrO$_2$ (ZrOCl$_2\cdot$8H$_2$O+ NH$_4$VO$_3$ solution), in the same experimental conditions as before and maintaining at 90 °C for 1h. The paste obtained after homogenization was dried at 120 °C until obtaining a solid. The latter samples were calcined at 550 °C for 12 h. The solids obtained were characterized by several techniques before being tested.

3.2. Characterization Methods

The powder XRD patterns were recorded at room temperature in the angular range 10–70° 2θ using a Brucker 5005 diffractometer (Billerica, MA, USA) equipped with equipped with a Cu Kα anode (λ = 1.54184 Å).

The specific surface area (SSA) evaluation, pore volume and mean pore diameter of the materials were performed by using N$_2$ adsorption−desorption isotherms on a Micromeritics ASAP 2020 Plus device. Prior to analysis, the samples were degassed under vacuum at 300 °C for 4 h, then the measurements were conducted at liquid nitrogen temperature ($-$196 °C). The SSA of catalysts was calculated from Brunauer−Emmett−Teller (BET) method. The Barrett−Joyner−Halenda (BJH) method was applied to the desorption branch to estimate the average pore radius in the range of mesopores. The total pore volume was measured as single desorption point, at p/p 0 = 0.99.

Fourier Transform Infrared spectra (FTIR) were recorded in the 4000 $-$400 cm^{-1} range using a VERTEX-70 spectrophotometer (Boston, MA, USA) with 4 cm^{-1} resolution.

Diffuse reflection UV-visible-NIR spectroscopy provides information on the degree of oxidation of metals transition, their coordination, and the environment symmetry. Spectra were recorded between 190 and 2500 nm using a Varian Cary 5E double monochromator spectrometer (Palo Alto, CA, USA) equipped with an integrating sphere. Polytetrafluoroethylene is used as a reference.

The scientific equipment QUATTRO S-FEG-Thermofisher (Waltham, MA, USA) is used for scanning electron microscopy (SEM) and energy dispersive X-ray analysis (EDX) to analyse morphology and composition as well as elemental mapping distribution.

ESR measurements were performed at 77K using a ESP 300 Bruker spectrometer (Billerica, MA, USA) working at 9.2 GHz (X band), using standard field modulation of 100 MHz and modulation width of 5 to 10 G.

3.3. Catalytic Activity

The 2-butanol dehydrogenation was performed as it has been described previously [39]. The 2-butanol conversion was studied in a U-shape fixed bed microreactor operating at atmospheric pressure. Before the reaction, the catalyst was sieved to a particle size range of 125–180 mm, then placed between two quartz wool plugs in the reactor, treated under air stream at 723 K for 2 h, and then cooled to the reaction temperature. Gaseous products

were analysed by chromatography on Chromosorb PAW (60/80 mesh) on a 4 m (1/8 inch) stainless steel column containing Carbowax 1500 (15%).

The oxidative dehydrogenation of propane (ODP) was carried out in the temperature range 723–823 K in a quartz U-shaped fixed bed microreactor functioning at atmospheric pressure. The feed mixture consisted of propane (6 vol%), O_2 (3 vol%) and N_2 (91 vol%), maintaining the total flow rate at 60 mL.min^{-1}. The outlet gas was analysed using two online chromatographs, the first for hydrocarbons separation on a Porapak Q column, equipped with a FID, and the second one equipped with a silica gel column and a TCD for the oxygenated products. Only propylene and COx were detected under selected test conditions.

Conversion of propane, 2-butanol, product selectivity, and turnover frequency of catalysts were determined as follows:

$$-conversion\,\% = 100 \times \frac{converted\ moles}{initial\ number\ of\ moles}$$
$$-selectivity\,\% = 100 \times \frac{moles\ of\ product}{converted\ moles}$$
$$-\text{yield}\,\% = 100 \times \frac{moles\ of\ product}{initial\ number\ of\ moles}$$
$$-Turnover\,frequency\,(s^{-1}) = \frac{F_{B0}X_A}{n_V},\ where\ F_{B0}: \text{Initial molar flow of } 2-butanol\ or\ propane;$$
$$X_A : product\ yield\ per\ g\ of\ catalyst;\ n_V : moles\ number\ of\ V, P\ per\ g\ of\ catalyst$$

4. Conclusions

Introducing different proportions of phosphate into the 3.6 wt%V_2O_5/ZrO_2 system significantly affected their structure and catalytic performance. Thus, the obtained results can lead us to draw the following conclusions:

- The introduction of vanadium and phosphate promote the tetragonal allotropic phase of ZrO_2.
- The most active catalyst corresponds to 3.6 wt% of V_2O_5/ZrO_2.
- The presence of phosphate improves the acid character of the 3.6 wt%V_2O_5/ZrO_2 system as found by dehydration of 2-butanol.
- The addition of phosphorus to V_2O_5/ZrO_2 increased selectivity.
- Good correlation between introduction phosphorus acidity and oxidative dehydrogenation of propane was found.
- The dehydration and dehydrogenation reactions activity of P loaded V_2O_5/ZrO_2 catalysts shows that it is a bi-functional system. V^{5+} ions appear to play a common role in both dehydration and dehydrogenation reactions.
- The insertion of P modifies the acidity of the system, coupled to the fact that P stabilizes the V^{4+}, leading to the formation of a redox couple responsible for dehydrogenation.

References

1. Sattler, J.J.H.B.; Ruiz-Martinez, J.; Santillan-Jimenez, E.; Weckhuysen, B.M. Catalytic Dehydrogenation of Light Alkanes on Metals and Metal Oxides. *Chem. Rev.* **2014**, *114*, 10613–10653. [CrossRef] [PubMed]
2. Farsad, A.; Lawson, S.; Rezaei, F.; Rownaghi, A.A. Oxidative dehydrogenation of propane over 3D printed mixed metal oxides/H-ZSM-5 monolithic catalysts using CO_2 as an oxidant. *Catal. Today* **2021**, *374*, 173–184. [CrossRef]
3. Gambo, Y.; Adamu, S.; Abdulrasheed, A.A.; Lucky, R.A.; Ba-Shammakh, M.S.; Hossain, M.M. Catalyst design and tuning for oxidative dehydrogenation of propane—A review. *Appl. Catal. A: Gen.* **2021**, *609*, 117914. [CrossRef]
4. Grabowski, R. Kinetics of Oxidative Dehydrogenation of C_2-C_3 Alkanes on Oxide Catalysts. *Catal. Rev.* **2006**, *48*, 199–268. [CrossRef]
5. Carrero, C.A.; Schloegl, R.; Wachs, I.E.; Schomaecker, R. Critical Literature Review of the Kinetics for the Oxidative Dehydrogenation of Propane over Well-Defined Supported Vanadium Oxide Catalysts. *ACS Catal.* **2014**, *4*, 3357–3380. [CrossRef]
6. Carter, J.H.; Bere, T.; Pitchers, J.R.; Hewes, D.G.; Vandegehuchte, B.D.; Kiely, C.J.; Taylor, S.H.; Hutchings, G.J. Direct and oxidative dehydrogenation of propane: From catalyst design to industrial application. *Green Chem.* **2021**, *23*, 9747–9799. [CrossRef]
7. Rase, H.F. *Handbook of Commercial Catalysts: Heterogeneous Catalysts*; CRC Press: Boca Raton, FL, USA, 2000.
8. Khodakov, A.; Olthof, B.; Bell, A.T.; Iglesia, E. Structure and Catalytic Properties of Supported Vanadium Oxides: Support Effects on Oxidative Dehydrogenation Reactions. *J. Catal.* **1999**, *181*, 205–216. [CrossRef]
9. Olthof, B.; Khodakov, A.; Bell, A.T.; Iglesia, E. Effects of Support Composition and Pretreatment Conditions on the Structure of Vanadia Dispersed on SiO_2, Al_2O_3, TiO_2, ZrO_2, and HfO_2. *J. Phys. Chem. B* **2000**, *104*, 1516–1528. [CrossRef]
10. Briand, L.E.; Tkachenko, O.P.; Guraya, M.; Gao, X.; Wachs, I.E.; Grünert, W. Surface-Analytical Studies of Supported Vanadium Oxide Monolayer Catalysts. *J. Phys. Chem. B* **2004**, *108*, 4823–4830. [CrossRef]
11. Bañares, M.A.; Martínez-Huerta, M.V.; Gao, X.; Fierro, J.L.G.; Wachs, I.E. Dynamic behavior of supported vanadia catalysts in the selective oxidation of ethane: In situ Raman, UV–Vis DRS and reactivity studies. *Catal. Today* **2000**, *61*, 295–301. [CrossRef]
12. Bañares, M.A.; Martínez-Huerta, M.; Gao, X.; Wachs, I.E.; Fierro, J.L.G. Identification and roles of the different active sites in supported vanadia catalysts by in situ techniques. In *Studies in Surface Science and Catalysis*; Corma, A., Melo, F.V., Mendioroz, S., Fierro, J.L.G., Eds.; Elsevier: Amsterdam, The Netherlands, 2000; Volume 130, pp. 3125–3130.
13. Burcham, L.J.; Deo, G.; Gao, X.; Wachs, I.E. In situ IR, Raman, and UV-Vis DRS spectroscopy of supported vanadium oxide catalysts during methanol oxidation. *Top. Catal.* **2000**, *11*, 85–100. [CrossRef]
14. Zhao, Y.; Qin, Z.; Wang, G.; Dong, M.; Huang, L.; Wu, Z.; Fan, W.; Wang, J. Catalytic performance of V_2O_5/ZrO_2–Al_2O_3 for methanol oxidation. *Fuel* **2013**, *104*, 22–27. [CrossRef]
15. Védrine, J.C. Heterogeneous Catalysis on Metal Oxides. *Catalysts* **2017**, *7*, 341. [CrossRef]
16. Bedia, J.; Rosas, J.M.; Márquez, J.; Rodríguez-Mirasol, J.; Cordero, T. Preparation and characterization of carbon based acid catalysts for the dehydration of 2-propanol. *Carbon* **2009**, *47*, 286–294. [CrossRef]
17. Soto, J.; Rosas, J.M.; Otero, J.C.; Rodríguez-Mirasol, J.; Cordero, T. Reaction Mechanisms of 2-Butanol Dehydration over a Phosphorus-Containing Activated Carbon Acid Catalyst. *J. Phys. Chem. C* **2018**, *122*, 16772–16778. [CrossRef]
18. Baertsch, C.D.; Komala, K.T.; Chua, Y.-H.; Iglesia, E. Genesis of Brønsted Acid Sites during Dehydration of 2-Butanol on Tungsten Oxide Catalysts. *J. Catal.* **2002**, *205*, 44–57. [CrossRef]
19. Rouimi, M.; Ziyad, M.; Leglise, J.J.P.R.B. Characterization and activity of CoMo/AlPO4 catalysts. *Phosphorus Res. Bull.* **1999**, *10*, 418–423. [CrossRef]
20. Kacimi, M.; Ziyad, M.J.J.C.P. Active sites in butan-2-ol conversion over magnésium and zinc phosphates. *J. Chim. Phys.* **1997**, *94*, 2007–2015. [CrossRef]
21. Brik, Y.; Kacimi, M.; Bozon-Verduraz, F.; Ziyad, M. Characterization of active sites on AgHf2(PO4)3 in butan-2-ol conversion. *Microporous Mesoporous Mater.* **2001**, *43*, 103–112. [CrossRef]
22. El Kabouss, K.; Kacimi, M.; Ziyad, M.; Ammar, S.; Ensuque, A.; Piquemal, J.-Y.; Bozon-Verduraz, F. Cobalt speciation in cobalt oxide-apatite materials: Structure–properties relationship in catalytic oxidative dehydrogenation of ethane and butan-2-ol conversion. *J. Mater. Chem.* **2006**, *16*, 2453–2463. [CrossRef]
23. Rajadhyaksha, R.A.; Knözinger, H. Ammonia adsorption on vanadia supported on titania—silica catalyst: An infrared spectroscopic investigation. *Appl. Catal.* **1989**, *51*, 81–92. [CrossRef]
24. Volpe, M.a.A. Partial oxidation of methane over VOx/α-Al_2O_3 catalysts. *Appl. Catal. A Gen.* **2001**, *210*, 355–361. [CrossRef]
25. Taghavinezhad, P.; Haghighi, M.; Alizadeh, R. Influence of aging temperature and Mg/Zr molar ratio on transformation of C_2H_6 to C_2H_4 over VOx catalyst supported on Mg–Zr nanocomposite. *Res. Chem. Intermed.* **2019**, *45*, 1907–1927. [CrossRef]

26. Čičmanec, P.; Ganjkhanlou, Y.; Kotera, J.; Hidalgo, J.M.; Tišler, Z.; Bulánek, R. The effect of vanadium content and speciation on the activity of VOx/ZrO2 catalysts in the conversion of ethanol to acetaldehyde. *Appl. Catal. A Gen.* **2018**, *564*, 208–217. [CrossRef]

27. El-Drissi, J.; Kacimi, M.; Loukah, M.; Ziyad, M.J.J.C.P. Activité0 de V_2O_5/TiO_2 modifié par le phosphore dans la réaction de déshydrogénation oxydante de l'éthane en éthylène. *J. Chim. Phys.* **1997**, *94*, 1984–1992. [CrossRef]

28. Khan, I.; Zada, N.; Khan, I.; Sadiq, M.; Saeed, K. Enhancement of photocatalytic potential and recoverability of Fe_3O_4 nanoparticles by decorating over monoclinic zirconia. *J. Environ. Health Sci. Eng.* **2020**, *18*, 1473–1489. [CrossRef]

29. Loukah, M.; Coudurier, G.; Vedrine, J.C.; Ziyad, M. Oxidative dehydrogenation of ethane on V- and Cr-based phosphate catalysts. *Microporous Mater.* **1995**, *4*, 345–358. [CrossRef]

30. Sadiq, M.; Bensitel, M.; Nohair, K.; Leglise, J.; Lamonier, C. Effect of calcination temperature on the structure of vanadium phosphorus oxide materials and their catalytic activity in the decomposition of 2-propanol. *J. Saudi Chem. Soc.* **2012**, *16*, 445–449. [CrossRef]

31. Wachs, I.E.; Weckhuysen, B.M. Structure and reactivity of surface vanadium oxide species on oxide supports. *Appl. Catal. A Gen.* **1997**, *157*, 67–90. [CrossRef]

32. Gao, X.; Jehng, J.-M.; Wachs, I.E. In Situ UV–vis–NIR Diffuse Reflectance and Raman Spectroscopic Studies of Propane Oxidation over ZrO_2-Supported Vanadium Oxide Catalysts. *J. Catal.* **2002**, *209*, 43–50. [CrossRef]

33. Védrine, J.C. Partial oxidation reactions on phosphate-based catalysts. *Top. Catal.* **2000**, *11*, 147–152. [CrossRef]

34. Vedrine, J.C. Acid and partial oxidation reactions on phosphorous-based catalysts. *Phosphorus Res. Bull.* **1999**, *10*, 37–48. [CrossRef]

35. Eon, J.G.; Olier, R.; Volta, J.C. Oxidative Dehydrogenation of Propane on γ-Al_2O_3 Supported Vanadium Oxides. *J. Catal.* **1994**, *145*, 318–326. [CrossRef]

36. Lewandowska, A.E.; Calatayud, M.; Lozano-Diz, E.; Minot, C.; Bañares, M.A. Combining theoretical description with experimental in situ studies on the effect of alkali additives on the structure and reactivity of vanadium oxide supported catalysts. *Catal. Today* **2008**, *139*, 209–213. [CrossRef]

37. Ternero-Hidalgo, J.J.; Guerrero-Pérez, M.O.; Rodríguez-Mirasol, J.; Cordero, T.; Bañares, M.A.; Portela, R.; Bazin, P.; Clet, G.; Daturi, M. Operando Reactor-Cell with Simultaneous Transmission FTIR and Raman Characterization (IRRaman) for the Study of Gas-Phase Reactions with Solid Catalysts. *Anal. Chem.* **2020**, *92*, 5100–5106. [CrossRef]

38. Ternero-Hidalgo, J.J.; Daturi, M.; Clet, G.; Bazin, P.; Bañares, M.A.; Portela, R.; Guerrero-Pérez, M.O.; Rodríguez-Mirasol, J.; Cordero, T. A simultaneous operando FTIR & Raman study of propane ODH mechanism over V-Zr-O catalysts. *Catal. Today* **2022**, *387*, 197–206. [CrossRef]

39. Elkabouss, K.; Kacimi, M.; Ziyad, M.; Ammar, S.; Bozon-Verduraz, F. Cobalt-exchanged hydroxyapatite catalysts: Magnetic studies, spectroscopic investigations, performance in 2-butanol and ethane oxidative dehydrogenations. *J. Catal.* **2004**, *226*, 16–24. [CrossRef]